Proceedings of the Korean Nuclear Society Autumn Meeting
Yongpyong, Korea, 2003

A Review on 3-D CFD Model Development for the CANDU-6 Moderator Analysis in KAERI

Churl Yoon, Bo Wook Rhee, and Byung-Joo Min

Korea Atomic Energy Research Institute
150 Dukjin-Dong, Yusong-Gu
Daejeon 305-353, Korea

ABSTRACT

A 3-D CFD model has been developed for predicting moderator temperature in the vicinity of the Calandria tubes under LOCA transients. Using the CFD model, a transient moderator analysis has done for the 35% RIH(Reactor Inlet Header) Breaks with loss of ECC(Emergency Core Cooling) Injection. During 40 sec after the break, local maximum subcooling near N17 channel was well bounded over 30^{o}C. Several aspects of future improvements on the CANDU moderator analysis model are mentioned, which include grid structure, hydraulic resistance correlation, and buoyancy force approximation. Some experimental works are also suggested.

1. INTRODUCTION

For some loss of coolant accidents with coincident loss of emergency core cooling in a CANDU-6 reactor, fuel channel integrity depends on the capability of the moderator to act as the ultimate heat sink. Under conditions of high-pressure tube temperature and high coolant pressure, the pressure tube could strain (i.e., balloon) to contact its surrounding Calandria tube. (PT/CT contact) Following contact between the hot pressure tube (PT) and the relatively cold Calandria tube (CT), there is a spike in heat flux to the moderator surrounding the Calandria tube, which leads to sustained CT dryout. The prevention of CT dryout following PT/CT contact depends on available local moderator subcooling. Higher moderator temperatures (lower subcooling) would decrease the margin of the Calandria tubes to dryout in the event of PT/CT contact. In CANDU safety analyses, it is one of major concerns to estimate the local subcooling of moderator inside the Calandria vessel under postulated accident scenarios.

The purposes of this study are to develop a 3-D CFD model for predicting the CANDU-6 moderator temperature, to analyze the moderator transient for 35% RIH break with loss of ECC injection, and to address some issues in the 3-D CFD model development. In this study, a three-dimensional CFD code, CFX-4, is used.

2. 3-D CFD MODEL FOR CANDU MODERATOR ANALYSIS

The reactor vessel of the CANDU-6 NPPs (Nuclear Power Plants) is an intended cylindrical tank (called 'Calandria') filled with moderator, which is 6 meters long with a diameter of 7.6 meters. The large cylindrical tank has eight inlet nozzles and two outlet ports, which are connected to two combined cooling loops. Inside the Calandria shell, there is a co-axial cylindrical core region with a smaller diameter. In the core region, a matrix of 380 pipes are located. The four inlet nozzles are located at the middle of each left and right sidewall, pointing upward. On the bottom of the large cylindrical tank, two outlet ports are located asymmetrically. Removing all the control mechanisms and monitoring devices, the simplified geometry for the moderator CFD analysis is shown in Fig. 1. Two closely located inlet nozzles are combined into a rectangular block. The standard k-ε turbulence model associated with logarithmic wall treatment is used to model turbulence generation and dissipation within the vessel. Buoyancy forces are modeled using the Boussinesq approximation in which the density is assumed to be a linear function of temperature.

The matrix of the Calandria tubes in the core region is simplified by the porous media approach (Todreas and Kazimi, 1990). The hydraulic resistance experienced by fluid flowing through the core region is accounted for as source terms of the momentum equations. The hydraulic resistance consists of two factors; form drag and friction drag. Neglecting the fact that hydraulic resistance is dependent on the attack angle between the flow direction and tube axis, the moderator fluid flow is conveniently decomposed into axial flow and lateral flow. For axial flow, there is no form drag. Thus, once we assume that we can decompose fluid flow into x, y, and z components, the hydraulic resistance of the axial flow could be expressed by the conventional correlations of frictional pressure loss in a cylindrical pipe. For the transverse (lateral) flow across the tube bank, Hadaller et al. (1996) investigated the pressure drop of fluid flows crossing staggered and in-line tube banks, in which the Reynolds number range is 2,000 to 9,000 and pitch to tube diameter ratio is 2.16. The obtained empirical correlation for the pressure loss coefficient (PLC) is expressed as

$$\mathrm{PLC} \equiv \frac{\Delta P}{N_r \cdot \rho \cdot \frac{V_m^{\,2}}{2}} = 4.54 * \mathrm{Re}^{-0.172}, \qquad (1)$$

where P = pressure (N/m^2),
N_r = number of rows, and
V_m = velocity before obstruction.

The steady state computation using CFX-4.4 was performed in an HP-C3600 workstation. The convergence criteria were the enthalpy residual reduction factor of 10^{-3} and the largest mass residual of 10^{-6}. Because the energy equation and momentum equations are strongly interrelated in this computation, the algebraic multi-grid solver and false time stepping technique were adapted to accelerate the converging speed for the energy equation. The number of steady computation iterations was about 200,000~300,000. The transient computation was performed in the same machine starting from the steady-state results, with time steps of 0.05 sec or 0.1 sec. For each time step, more than 100 iterations were required to reach the enthalpy residual reduction factor of 10^{-3} and the mass residual of 10^{-5}.

Under normal operating conditions, the calculated maximum temperature of the moderator is 82.9 ^{o}C at the upper center region of the core, which corresponds to the minimum subcooling of 24.8 ^{o}C. In Figs. 2(a) and 2(c), flow reversal is observed only for the injected fluid from the inlet nozzle far from the outlet port. The cold injected fluid from the other side inlet nozzle goes all the way through the upper reflector region, guided by the upper circumferential vessel wall. The two injected fluids meet together at the angle of about 50^{o} over the horizontal centerline, where the jet reversal occurs. The reversed fluid goes down to the bottom, guided by the circumferential lower vessel wall. This asymmetry of flow pattern is induced by the interaction between the buoyancy forces and the inlet jet momentum forces. The velocity vectors in the core region are relatively small compared to those of the reflector region due to the hydraulic resistance in the core region. In Figures 2(a) and 2(c), the temperature distribution shows a steep change of temperature around the jet reversal area. In this area, the fluid from the opposite side nozzle heated during travel suppresses the cold injected fluid. The hottest spot is located at the upper center area of the core region, which slightly tilts to one side from the vertical centerline.

The transient condition starts after the 35% reactor inlet header(RIH) break with Loss of ECC Injection, which gives the highest heat load to moderator among all LOCA's. The initial condition for the transient analysis is the steady-state solution. From the Large LOCA analysis, CATHENA predictions (0 to 40 s) and CHAN predictions (after 40 s) gave the results that some of the pressure tubes in the critical pass (i.e. downstream of the break) contact with the Calandria tubes from 20 to 40 seconds, and then are followed by the rest of the pressure tubes in the broken loop between 40 and 2000 seconds. The CHAN results also indicated that a 35% RIH break with steam flow = 10 g/s gave the largest power to moderator following PT/CT contact. For this reason, the moderator temperature transient will be done for steam flow of 10 g/s after 40 sec. Note that the Class IV power is available for this analysis. The moderator analysis for LLOCA/LOECC without Class IV power will be performed in the future researches.

The heat sources of moderator during this transient are divided into the heat load due to fission product decay and neutronic power, and the heat load due to PT/CT contact. The transient consists of a Blowdown Phase (0 to 40 sec) and a Post-Blowdown Phase (after 40 sec). Fig. 3 shows the total heat load to moderator and the power to the heat exchangers for a 35% RIH with Loss of ECC injection. The moderator heat load curve has three distinct humps, which are due to the LOCA power pulse at around 1 sec, the number of PT/CT contacts in the critical pass at 20~40 sec, and the contacts of the rest of the pressure tubes in the broken loop after 40 sec. For the case of Class IV power available, the heat removed by the heat exchangers exceeds the heat input shortly after reactor trip. It leads to a continuous decrease in the average moderator temperature.

The minimum subcooling over the full domain inside the Calandria vessel and the local subcooling at the location of N16 channel are displayed along transient time in figure 4. The minimum subcooling occurs at the upper corners of the Calandria subshell. The saturation temperature at this location is hydro-statically calculated to be 107.67^{o}C, when the cover gas pressure is 18.0 kPa(g) and density of moderator is 1084.7 kg/m^{3}. Similarly, the saturation temperature at N16 location is 115.02^{o}C. Because of the lower saturation temperature at the upper corners of subshells, the minimum subcooling over the domain occurs at the subshells

even though the highest temperature sometimes appears in the core region during the transient. The minimum subcooling increases continuously due to the decrease of total heat load to moderator during the transient. The solid red line in Fig. 4 is local subcooling of N16 channel surface, where the highest temperature appears. The power pulse at around 2sec induces an instant decrease of the N16 local subcooling. The N16 local subcooling increases gradually after 3 sec until 20 sec, when the local subcooling of N16 channel goes down due to PT/CT contacts. Consequently, the local subcooling in the core region is well bounded over the minimum subcooling of 30^{o}C, where the film boiling can occur in a certain condition.

3. SPECIAL TOPICS

A modeling procedure follows the steps from easy to difficult, from basic to high-tech, and from simple to complex. Some methods of the current moderator analysis model are primitive. To improve the accuracy and ability of the model, several special topics are considered in this section.

Grid Structure Selection

The principles of generating the optimum grid structures for CANDU-6 moderator circulation analysis are as followings. Firstly, do not violate the assumptions of porous media approach, which means that the grid size should be large enough to contain uniform portions of fluid and solid structures in porous region. Secondly, insert more cells in the reflector region and downstream of inlet jets to reduce the discretization errors. And finally, make the inlet nozzle grids as close to the real geometries as possible, because the moderator circulation is basically induced by the interaction of inlet jet momentum forces and buoyant forces and is largely affected by inlet jet characteristics.

In the current Wolsong 2/3/4 moderator simulations, the ‘radial-shaped’ grid structures were used as shown in Fig. 5. With the radial-shaped grid structures, some problems raised such as relatively small grid sizes near the center region and large grid sizes in the reflector region. The suggested grid structures, that are so called “butterfly-shaped”, are shown in Fig. 6. Note that cell sizes in the core region are larger than those of Fig. 5, and that cells in reflector region are smaller than those of Fig. 5 for the case of the same number of total cells.

The butterfly-shaped grid is composed of four solid blocks. 3-D solid patches are inserted at each inlet nozzle location, and 2-D surface patches are inserted representing nozzles surfaces. The total number of cells is 38,272, which is ~1.96 times more than the radial-shaped grid (19,504). The number of cells in z-direction is also larger than that of the old radial-shaped grid, to enable the implementation of the more specific inlet velocity profiles. The YPLUS value of the near-most cell centroids at the circumferential wall is 30 ~ 100. The moderator analysis with the new butterfly-shaped grid is in progress.

Error of Boussinesq Approximation

The Boussinesq approximation is widely used for buoyancy force of incompressible flow. This approximation is valid when Mach number is less than 0.1 and temperature variation is

relatively small (that is, $\beta(T - T_{ref}) < 0.1$). The CANDU moderator analysis results are affected mainly by the interaction between the momentum force of inlet jets and the buoyant force in the core region. In the temperature range of 45°C ~ 85°C over the whole domain, thermal expansion coefficient varies from 3.8×10^{-4} to 6.6×10^{-4}. But, thermal expansion coefficient barely changes due to the static pressure change (120 kPa ~ 200 kPa). In this section, the accuracy of Boussinesq approximation will be re-considered.

The general y-momentum equation for the incompressible steady flow with constant properties and –y directional gravitational force is

$$\rho\left(u\frac{\partial u}{\partial x} + v\frac{\partial v}{\partial y} + w\frac{\partial w}{\partial z}\right) = -\frac{\partial P}{\partial y} + \mu\nabla^2 v - \rho g \quad . \tag{2}$$

Here, the buoyancy term is simply expressed as ρg . One can re-write density with respect to a reference density ρ_0.

$$\rho = \rho_0 + (\rho - \rho_0) \tag{3}$$

The $\rho_0 g$ part is absorbed into the pressure gradient, so the buoyancy term in y-momentum equation becomes

$$\vec{S}_{M,buoy} = (\rho - \rho_0)\vec{g} \quad . \tag{4}$$

In the Boussinesq approximation, it is assumed that the densities of other terms are constant density ρ_0, and that the density of buoyancy term is a linear function of temperature.

$$\rho - \rho_0 = -\rho_0 \beta (T - T_0) \tag{5}$$

Here, the thermal expansion coefficient β is defined as

$$\frac{\upsilon}{\upsilon_0} = 1 + \beta\Delta T \tag{6}$$

or $$\beta = -\frac{1}{\rho}\frac{d\rho}{dT} = \frac{1}{\upsilon_0}\frac{d\upsilon}{dT} \tag{7}$$

By using the D_2O property data of the CATHENA code, the density of heavy water is plotted in Fig. 7 as a function of temperature within the CANDU moderator temperature range. For the pressure range of 1 atm ~ 2 atm, the effects of pressure change are almost negligible. Figure 8 shows the thermal expansion coefficient of D_2O, calculated from Eq. (7) at the pressure of 160 kPa. While the constant β value of Boussinesq approximation in the current moderator analysis is chosen as 0.000504 K^{-1}, the actual β value varies within the range of 0.00035 ~ 0.00065 K^{-1}. The β value at 85°C is almost twice the β value at 40°C.

The density errors of the Boussinesq approximation are smaller than 0.2 % within the temperature range, and can be neglected. But, when the density is inserted into the buoyancy source term as a form of density difference or temperature difference, the error amplifies itself. Table 1 presents the error of buoyancy term between the Boussinesq approximation (5)

and (4). The error of buoyancy term goes up to 18 % with the Boussinesq approximation. Therefore, a trial to use (4) directly instead of using the Boussinesq approximation is in progress.

Effect of Outlet Position

It is well known that the CANDU moderator circulation pattern is not symmetric under normal operating conditions due to the interaction of the momentum force of inlet jets and the buoyancy force in the core region. This phenomenon is not clearly caused by the geometric asymmetry, because even in a symmetric experimental facility the moderator circulation is not symmetric under the condition that the momentum-to-buoyancy force ratio is similar to that of the operating condition of real CANDU reactor vessel. Then, a new question arises in mind. "Which factor determines the location of the hotter side and the cooler side?" In the simulation of symmetric moderator circulation facility, the determinant factor to affect the direction of hotter/cooler side is thought to be numerical perturbation like sweeping direction. But, in the simulation of real CANDU moderator circulation, does the geometric asymmetry play any role on the determination of hotter/cooler side? The asymmetry of real CANDU moderator circulation is represented by the location of outlets. Therefore, the two simulation results are compared with different outlet positions: one in "B" side and another in "D" side in Fig. 1.

The moderator analyses with "B" side outlets have been performed so far, which is the analysis for real CANDU geometry. Another moderator analysis with "D" side outlets is performed in this study. The results with "D" side outlets show mirror images of Fig. 2. The direction of asymmetric flow pattern was determined by the outlet position. That is, the maximum temperature appears in the "B" side for the moderator circulation with "B" side outlets, and the maximum temperature appears in the "D" side for the moderator circulation with "D" side outlets. The results with "D" side outlets are not presented in this paper.

As a conclusion, one can say that the main factor that determine the direction of asymmetric flow pattern is the location of outlets, even though it is usually known that downstream condition does not affect to the upstream.

Improvement of Empirical Hydraulic Resistance Correlation in Porous Media

In this model, the hydraulic resistance in the core region is simply decomposed into axial flow and lateral flow. For axial flow, there is no form drag. Thus, once when we assume that we can decompose fluid flow into x, y, and z components, the hydraulic resistance of axial flow could be expressed by the conventional correlations of frictional pressure loss in a cylindrical pipe. Friction factor, f , is calculated from the friction factor correlation for the flow inside circular pipes. For the turbulent flow of a low Reynolds number,

$$R_z = \left.\frac{\Delta P}{\Delta L}\right)_z = \frac{\Delta P_{fric}}{\Delta z} = \frac{f\rho\, u_z^2}{2D_e} \tag{8}$$

$$f = 0.316 \cdot \mathrm{Re}^{-0.25} \tag{9}$$

Here, Reynolds number Re is defined by $u_z D_e / \nu$.

For the transverse(lateral) flow across the tube bank, the obtained empirical correlation for the pressure loss coefficient is expressed by using the correlation (1) (Hadaller et al., 1996). The hydraulic resistance source term in momentum equations are in a form of pressure drop per unit length.

$$\frac{\Delta P}{\Delta L} = \frac{N_r}{\Delta L} 4.54 \cdot \mathrm{Re}^{-0.172} \cdot \rho \cdot \frac{V_m^{\ 2}}{2} \tag{10}$$

Here, $N_r / \Delta L$ can be expressed as an inverse of the pitch of the tube bank and the Reynolds number is defined as $V_m D / \nu$. Note that V_m is the velocity before entering the tube bank and that V_m is different from the local moderator velocity in the core region of CANDU calandria vessel, V_c. And the surface porosity (permeability) is defined as the ratio of the area occupied by fluid A_f to the total area A_T.

$$V_m = \gamma_A V_c \tag{11}$$

$$\gamma_A \equiv \frac{A_f}{A_T} \ . \tag{12}$$

The final formulation of transverse(lateral) pressure drop per unit traveling length is expressed as

$$\left.\frac{\Delta P}{\Delta L}\right)_i = \frac{1}{p} 4.54 \cdot \left(\frac{\gamma_A V_c D}{\nu} \right)^{-0.172} \cdot \rho \cdot \frac{\left(\gamma_A^{\ 2} V_c\right)}{2} u_i \,, \tag{13}$$

where subscript i denotes x or y component.

From Eq. (8) & (9) and from Eq. (13), it is appear that the hydraulic resistance is not proportional to the square of velocity magnitude. Therefore it is clear that the decomposition induces some error in the calculation of hydraulic resistance. To adjust this problem, some consideration of the angle between flow directions and the Calandria tube array will be added in the hydraulic resistance model for the core region.

Figure 9 shows the temperature effect on the pressure drop per unit traveling length. Heating-up reduces the flow resistance and cooling-down increases the impedance. Because the fluids are heated up during traveling across the core region, temperature effect must be considered in the implementation of hydraulic resistance.

4. REQUIRED EXPERIMENTAL WORKS

In Canada, many experimental works have been performed to understand various phenomena of the CANDU moderator circulation. But, the CANDU moderator analysis in Korea was start-up just couple of years ago, so that any valid experimental data is not available. Some limited experimental data were collected through open literatures, which is not quite enough even for validation of the developed models. In this section, couple of

experimental studies is suggested for the model development.

Small Scaled 3-D Moderator Circulation Experiment

A small-scaled 3-D moderator circulation experiments are planned in Handong University by KINS. These experimental data will be used for the validation of analytical models for moderator temperature prediction.

Velocity Profiles at Inlet Nozzles

The inlet jet momentum forces initiate the moderator circulation. The developed model adapted uniform normal velocity condition at the inlet boundary conditions. Actual velocity profile can be only obtained by a experimental studies, because the geometry of inlet nozzles is very complex. The secondary flow in the connected pipes as well as the inlet nozzle geometry determines the velocity profiles at inlet nozzles. If a scaled facility is used, geometric similarity should be maintained to get meaningful data. Figure 10 shows an inlet nozzle of the CANDU-6 moderator system. The essential factors of this experiment are: exact (scaled) geometry, geometric similarity, scaling technique, and decent detecting technique to get 3-D velocity profiles.

5. ADDITIONAL COMMENTS

Under steady-state normal operating condition, about 80% of the total heat dumped into the moderator is generated by direct heating of γ-ray and neutrons and the rest is generated by the convective heating through the Calandria tube walls. When one ignore this fact and assume that all the heat is transferred by convective heating through the tube walls, fluctuating fluid temperature and velocity fields are observed in numerical simulations as well as experiments. This phenomenon is observed in the core region, because the direction of the buoyancy force is counter-current. From computational experiments, the period of fluctuation was about 10 sec, and the temperature deviation was ~3^{o}C with heating only by convective heat transfer. If this is the same as real phenomena, some uncertainty should be added to the steady results from the current model, because the current model adapts the porous media approximation and consequently 100% direct heating. More study is needed for this problem.

REFERENCES

1. N.E. Todreas and M.S. Kazimi, *Nuclear System II: Elements of Thermal Hydraulic Design*, Chap.5, Hemisphere Publishing Corporation, 1990.
2. G.I. Hadaller, R.A. Fortman, J. Szymanski, W.I. Midvidy and D.J. Train, "Fricktional Pressure Drop for Staggered and In Line Tube Bank with Large Pitch to Diameter Ratio," Preceedings of 17th CNS Conference, Federiction, New Brunswick, Canada, June 9-12, 1996.
3. *CFX-4.2: Solver Manual*, CFX International, United Kingdom, December 1997.

4. C. Yoon, B.W. Rhee, and B.J. Min, "Validation of CFD Analysis Model for the Calculation of CANDU6 Moderator Temperature Distribution," Proceedings of the KSME 2001 Fall Annual Meeting B (Korean), 499-504, Nov. 2001.
5. S.-O. Yu, Y.-S. Jung, M. Kim, and H.-J. Kim, "Safety Assessment of Generic Safety Issues for CANDU-6 Reactors: Analyses of Moderator Heat Sink Integrity," Proceeding of the Korean Nuclear Society Spring Meeting, Gyeongju, Korea, May 2003.

Table 1: Error Estimation of Buoyancy Term in Y-Momentum Equation

$T_0 = 59.31\ ^oC$, $\rho_0 = 1090.97\ kg/m^3$, $\beta = 0.000505/^oC$				
Temp. [^{o}C]	Density [kg/m^3]	$\Delta\rho = \rho - \rho_0$ **A**	Boussinesq App. $\rho_0\beta(T - T_0)$, **B**	$\frac{\lvert A - B \rvert}{A}$
40.35	1099.85	8.88	10.44	0.1751
45.08	1097.92	6.95	7.84	0.1262
49.82	1095.79	4.83	5.23	0.0829
55.75	1092.86	1.89	1.96	0.0352
59.31	1090.97	0	0	0
65.26	1087.59	-3.37	-3.27	0.0284
70.02	1084.70	-6.26	-5.90	0.0574
74.80	1081.66	-9.30	-8.53	0.0827
80.77	1077.66	-13.30	-11.82	0.1113
85.56	1074.30	-16.66	-14.46	0.1323

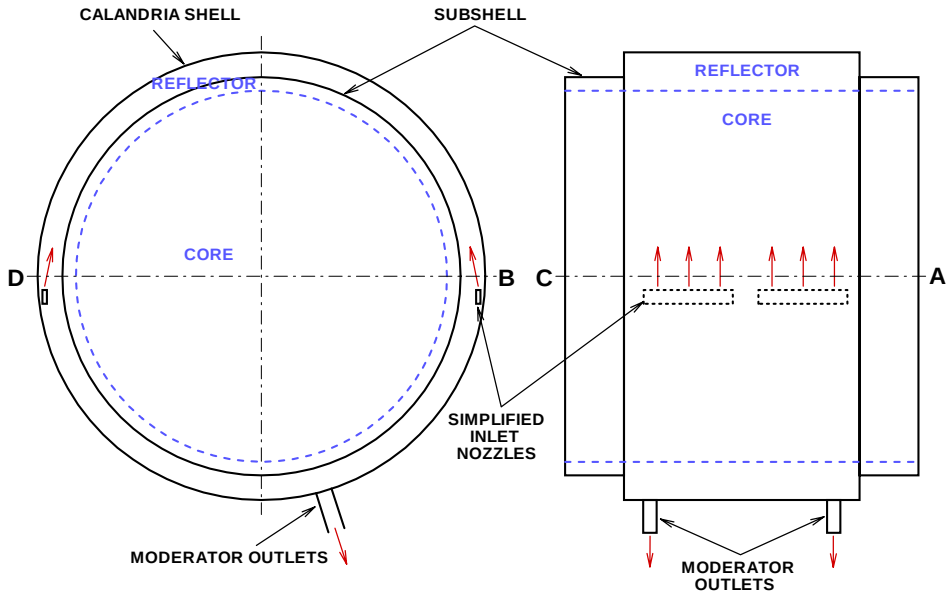

Figure 1: Simplified geometry of the CANDU Calandria vessel for moderator analysis

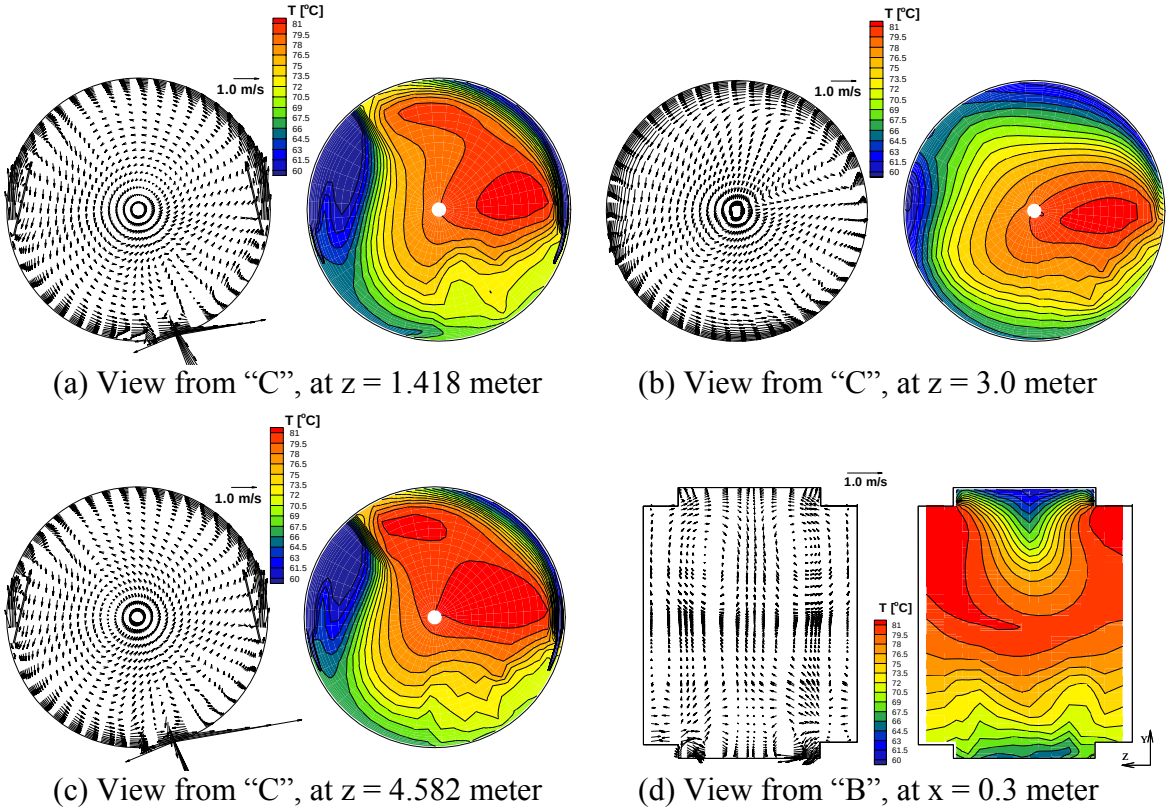

(a) View from "C", at z = 1.418 meter

(b) View from "C", at z = 3.0 meter

(c) View from "C", at z = 4.582 meter

(d) View from "B", at x = 0.3 meter

Figure 2: Velocity fields and temperature distributions of CANDU-6 moderator under normal operating conditions

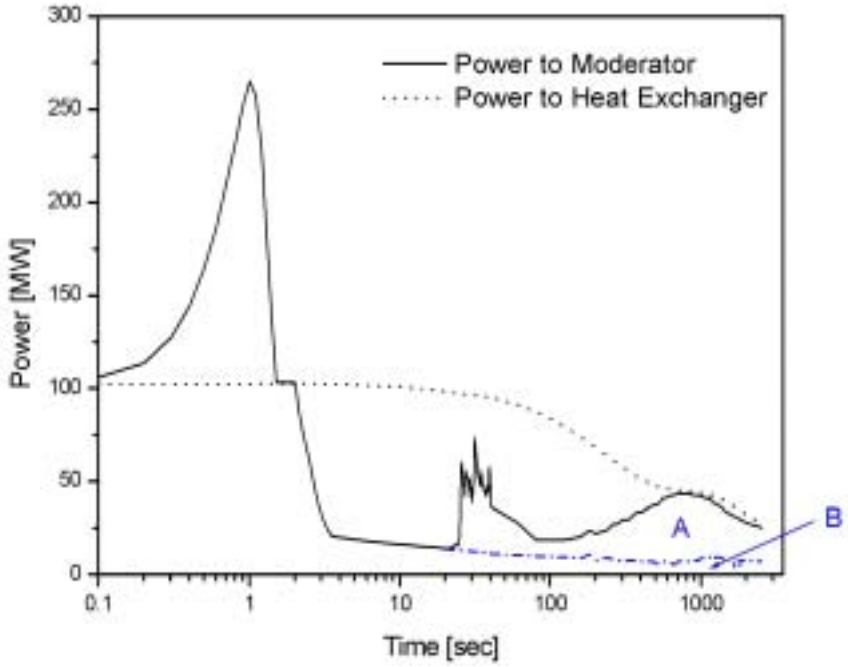

Figure 3: Total power to moderator and power to heat exchanger for 35% RIH with Loss of ECC injection

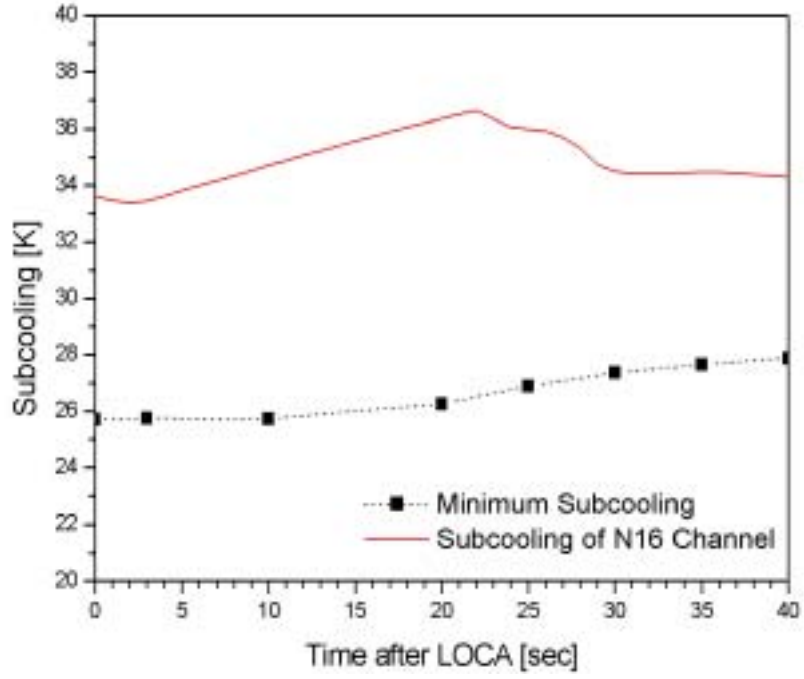

Figure 4: Minimum subcooling of moderator and local subcooling at the location of N16 channel

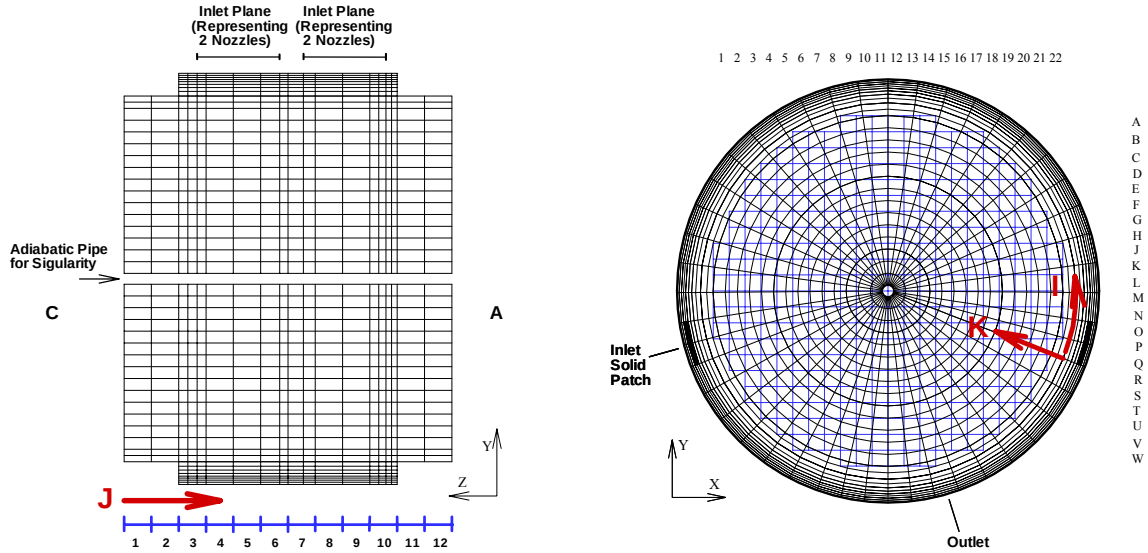

(a) Y-Z plane (View from "B") (b) X-Y plane (View from "C")

Figure 5: Radial-shaped grid structure and channel-bundle locations

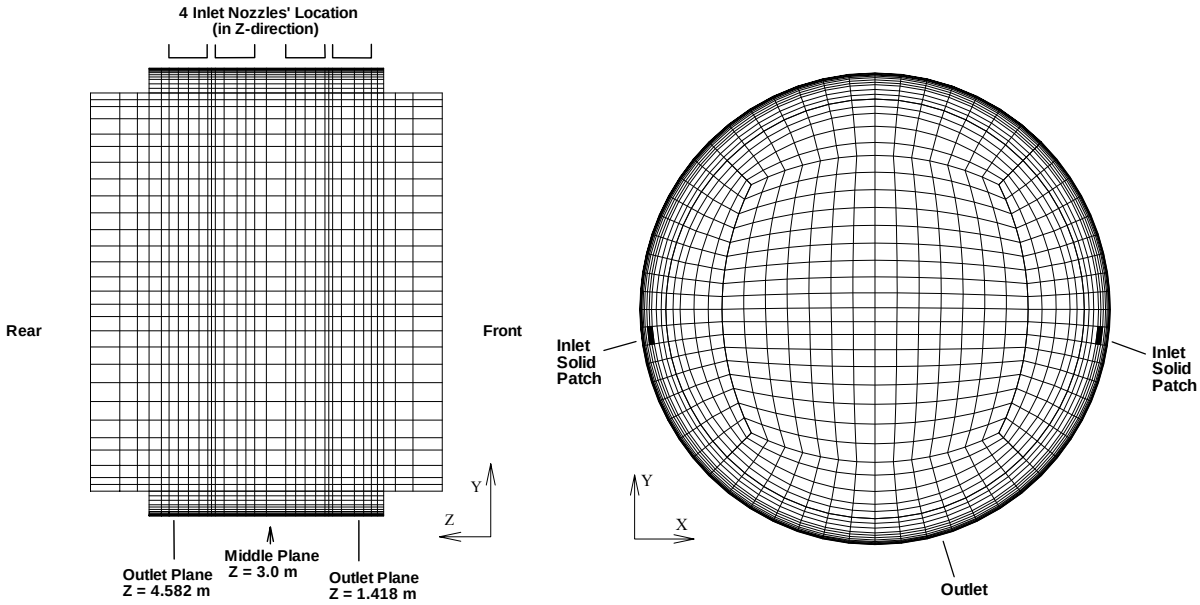

(a) Y-Z plane (View from "B") (b) X-Y plane (View from "C")

Figure 6: Butterfly-shaped grid structure and channel-bundle locations

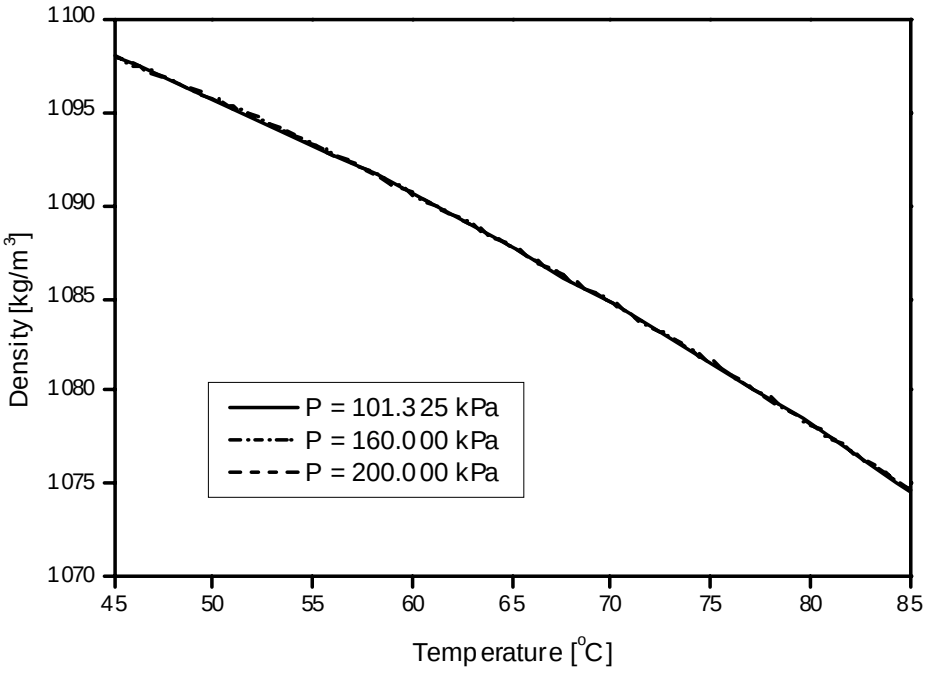

Figure 7: D_2O density variation according to temperature change for the pressure of 1~2 atm

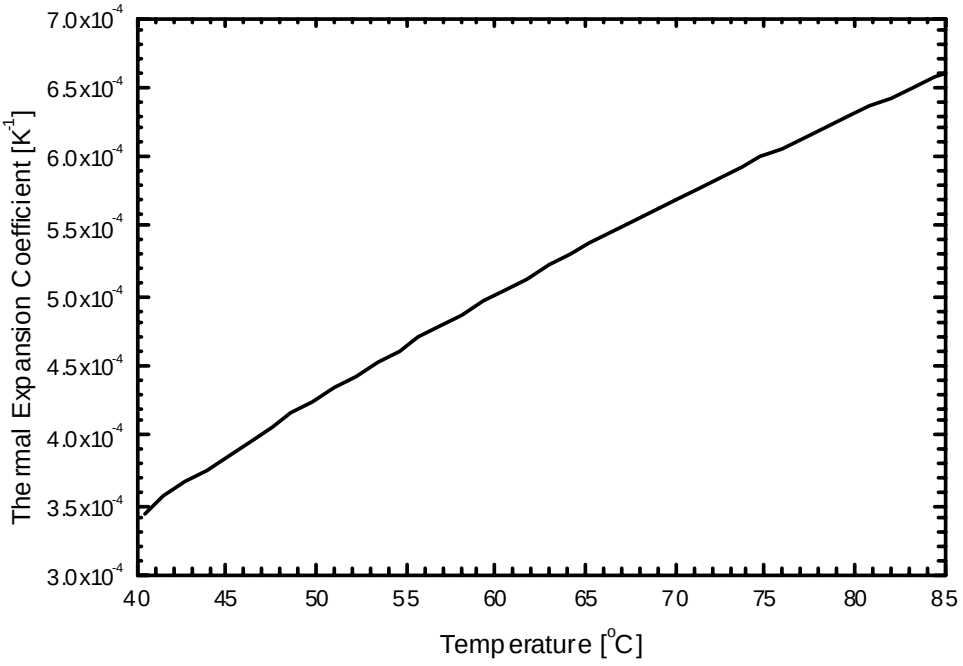

Figure 8: Thermal expansion coefficient of D_2O within a certain temperature range at 1.5 atm

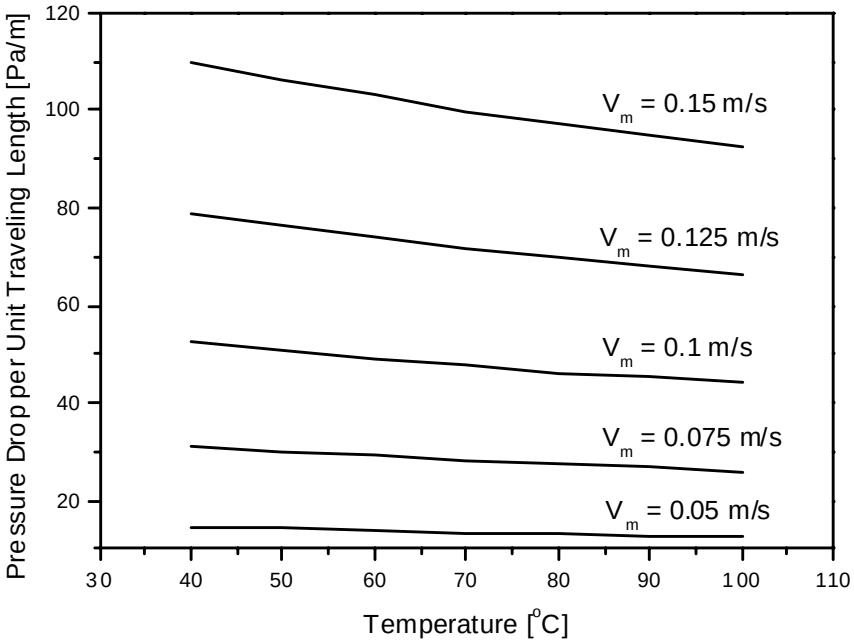

Figure 9: Temperature Effects on the Pressure Drop per Unit Traveling Length

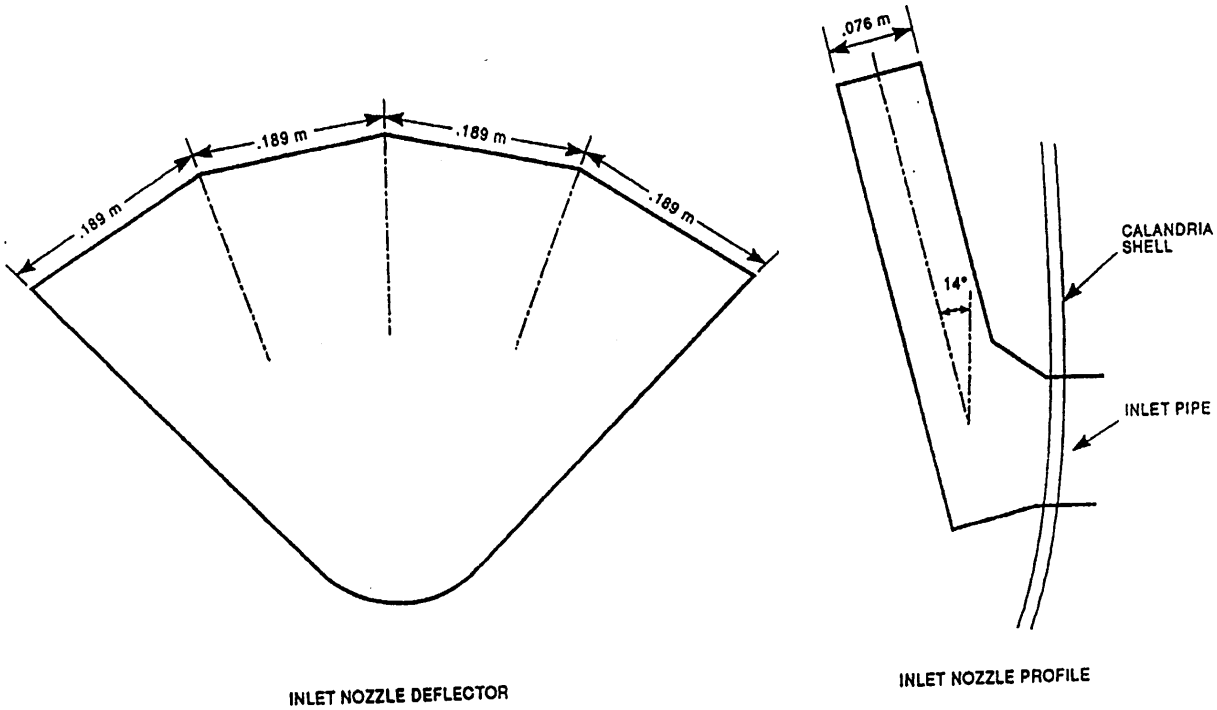

Figure 10: Inlet nozzle of the CANDU-6 moderator system